

Low-temperature structure of S/Cu(111)

Erik Wahlström, Inger Ekvall, Theresa Kihlgren, Håkan Olin, Stig-Åke Lindgren, and Lars Walldén
Physics and Engineering Physics, Chalmers University of Technology and Göteborg University, SE-412 96 Göteborg, Sweden
 (Received 13 February 2001; revised manuscript received 21 May 2001; published 24 September 2001)

We use scanning tunneling microscopy (STM) and core and valence photoemission as well as low-energy electron diffraction to characterize recently discovered S/Cu(111) surface structures that appear at low coverage below ordering temperatures of around 230 K. At even lower coverage ordered local arrangements are observed near steps and dislocations. Of the laterally extending structures one is open and honeycomb (hc) like, while three other structures (I,II,III) are more complicated. It is suggested that the structures can be explained as reordered (0001) planes of CuS. Surprisingly the open hc structure gives room for the Cu(111) surface state according to photoemission and scanning tunneling spectra. Core level spectra provide support for one of the models proposed for an earlier studied room-temperature structure [Cu(111)-($\sqrt{7} \times \sqrt{7}$) $R \pm 19.1^\circ$ -S].

DOI: 10.1103/PhysRevB.64.155406

PACS number(s): 79.60.Dp, 68.37.Ef

I. INTRODUCTION

In path-breaking studies Hasegawa and Avouris¹ and Crommie *et al.*² showed that scanning tunneling microscopy (STM) can be used to image the standing waves formed by electrons scattered by defects such as steps or impurities on Au(111) and Cu(111) surfaces. In one case circular standing waves were observed around unidentified impurities in the Cu(111) surface.² It is known that S can be brought to the surface by heating copper³ and this atom might therefore be at the center of the ring-shaped standing-wave pattern observed in STM. When several such patterns are observed in one image it was noted that the distances between the centers are given by multiples of half the Fermi wavelength as should be the case for an adatom interaction mediated by the surface electrons.⁴ To perform more controlled experiments it was found desirable to deposit known atoms on the surface. We have therefore deposited S atoms on the surface by exposing it to H₂S, but this has in no instance produced images with lateral standing waves around adsorption-induced point defects.

The experiments have, however, revealed a number of low-temperature S/Cu(111) structures which are described in the present paper. In a previous Brief Report details, which will not be repeated here, were given about one of the structures.⁵ At low surface coverage the only sign of an adsorbed species is that step edges between terraces are reordered and become decorated by defects. As the deposition is continued a series of S/Cu(111) structures forms, which have been studied since for a long time with a number of different methods. Using low-energy electron diffraction (LEED) Domange and Oudar observed a split ($\sqrt{3} \times \sqrt{3}$) $R \pm 30^\circ$ structure, and upon further deposition a complex undetermined structure and finally a ($\sqrt{7} \times \sqrt{7}$) $R \pm 19.1^\circ$ structure.⁶ Numerous later experiments followed and have given further details concerning the three structures.^{7-11,5,12,13} The complex structure develops at $\theta \sim 0.35$ and can be denoted as $\lfloor \begin{smallmatrix} 4 & 1 \\ -1 & 4 \end{smallmatrix} \rfloor$, where θ is the surface density of S, given in units of the surface atomic density of Cu(111). The complex structure is sometimes labeled the zigzag structure due to the characteristic zigzag lines observed by STM.^{10,11} If the temperature

is raised to ~ 400 K, a reversible phase transition is observed from the zigzag pattern to a split ($\sqrt{3} \times \sqrt{3}$) $R \pm 30^\circ$ pattern.⁸ At a coverage of $\theta \sim 0.4$ islands of the ($\sqrt{7} \times \sqrt{7}$) $R \pm 19.1^\circ$ structure form in the zigzag structure at room temperature (RT).¹⁰ At the saturation coverage of 0.43 for H₂S deposition of S, the whole surface is covered with the ($\sqrt{7} \times \sqrt{7}$) $R \pm 19.1^\circ$ structure. The same structure can also be found for other close-packed metal surfaces as for S/Ag(111),¹⁴ S/Pd(111),^{15,16} and S/Ru(0001).¹⁷

Most studies performed earlier have been devoted to studying structures observed when the sample is kept at or above RT. In the new structures reported on here the S content is lower than in the previously studied ones and they are observed only at low temperature.⁵ Some characteristics of the structure with the lowest S content, labeled the honeycomb (hc) structure, were described previously. In STM images it is characterized by an open honeycomb pattern of protrusions and it has a large ($\sqrt{43} \times \sqrt{43}$) $R \pm 7.5^\circ$ unit cell.

Presumably the low- T structures are formed by an adsorbed species that at RT is disordered and too mobile on the surface to be imaged by STM. The identity of this species and whether it remains intact upon ordering are of interest. Recently, based on theoretical calculations, Feibelman suggested that S-decorated Cu trimers are a likely agent of S-enhanced transport between islands on Cu(111).¹⁸ A planar Cu₃S₃ cluster was suggested as the carrier. The formation energy is low and the cluster is predicted to be mobile on the surface. The low- T structures may thus be built of units of interest for understanding the role of S atoms in the diffusion process.

Another reason for interest in the new structures is that the combination of low disordering temperature, large unit cell, and open character suggests that long-range forces between the building units can be important. Such forces can be mediated by the electrons in the substrate surface. It is therefore of interest to find out to what extent the electronic structure of the Cu(111) surface is modified in the low- T structures. To this end we have used valence and core level photoemission and performed scanning tunneling spectroscopy (STS). In the discussion of the results we note that the structures have a likeness to that of bulk CuS (covellite). In

addition to the extended structures we report on decoration of step edges and dislocations which have a local 2×2 ordering.

II. EXPERIMENT

The STM experiments were made with an ultrahigh-vacuum variable-temperature STM (Omicron Vakuumphysik GmbH) equipped with LEED optics. The base pressure was in the 10^{-11} mbar range. The tip preparation procedure has been described elsewhere.¹⁹ The images were acquired in constant-current mode and are presented with protruding features brighter. The bias voltage U refers to the potential difference between the sample and the tip. STS was performed by current imaging tunneling spectroscopy. The feedback loop was turned off, the scanning stopped, and I/V curves acquired. The core level photoemission experiments were performed in MAX-lab (Lund University) at BL I311, while the valence photoelectron spectra were recorded at BL 52.

The substrates were cut from the same piece of single crystal, mechanically polished and electropolished before insertion into the vacuum systems. The final preparation was made by repeated cycles of sputtering with Ne^+ or Ar^+ at an ion energy of ~ 800 eV and annealing at ~ 700 K.

To deposit sulfur the Cu surface was exposed to H_2S at RT. H_2S adsorbs dissociatively forming H_2 and S, and at RT H_2 desorbs readily, leaving only sulfur at the surface.⁸ The θ values are obtained using the coverage of $\theta=0.35$ as reference for the zigzag structure.^{8,7} In addition to this we assume that the sticking coefficient is constant for $\theta < 0.35$. Support for this is given by Auger intensity studies.⁸ Furthermore we find that the S $2p$ core level intensity increases linearly with exposure in this range.

III. RESULTS

A. STM-LEED results

1. Clean Cu(111)

STM images of the clean Cu(111) surface show the characteristic close-packed ordering with a nearest-neighbor distance of 2.55 \AA . The used crystal had a noticeable density of dislocations at the surface, which are identified as simple dislocations, i.e., edge and screw dislocations. The dislocations induce a detectable height distortion in the surrounding lattice ranging $100\text{--}300 \text{ \AA}$ away from the center of the defect (the extension of the dislocations can be seen in Fig. 1).

2. S/Cu(111): Room temperature

At $\theta > 0.05$ there are noticeable changes in the images. Atomic resolution imaging is possible, but much harder to obtain than for the clean surface. The lattice resolved is that of Cu(111). A drastic change is that step edges are aligned along the $\langle 110 \rangle$ directions. Furthermore, the step edges and dislocations are decorated by protrusions, separated by 5.1 \AA , twice the interatomic distance of the Cu atoms. At some of the step edges and dislocations the decorations form equilateral triangles, with an average side length of $\sim 30 \text{ \AA}$. The triangles enclose an area of protrusions in 2×2 order

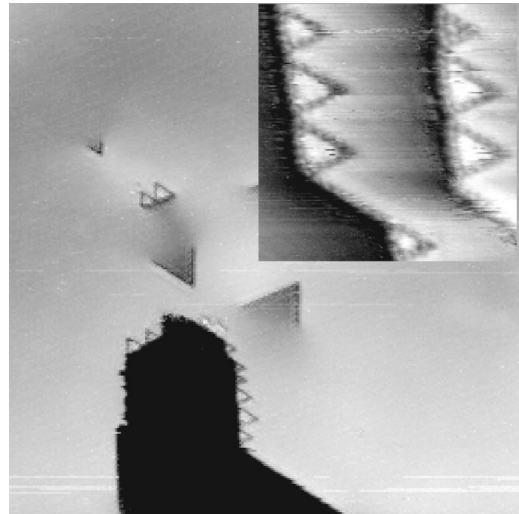


FIG. 1. S/Cu(111) at $\theta \sim 0.1$. The dislocations (short straight lines and V shapes) distort the lattice even far from imperfections (height differences $\sim 0.1 \text{ \AA}$). Some defects are decorated by sulfur structures (triangles). The inset shows a closeup of steps which are decorated by triangles and protrusions. $U = -0.946 \text{ V}$, $I = 0.456 \text{ nA}$, $T = 300 \text{ K}$, $1000 \times 1000 \text{ \AA}^2$ (inset $120 \times 120 \text{ \AA}^2$).

(Fig. 1). The brightness of the center part of a triangle indicates that it is higher than the surrounding terrace (Fig. 1). At RT the protrusions do not immobilize the step edges since new step positions can be seen in consecutive images.

3. S/Cu(111): Low temperature

a. $\theta < 0.25$. When the temperature is lowered at low coverage ($\theta < 0.05$) no drastic changes are noted. The edges and dislocations are still decorated. We do not observe any changes within the time of the experiment (~ 30 min) in the positions of the protrusions. A significant change at higher coverages is that new structures are formed close to dislocations (Fig. 2) and step edges. They appear as protruding chains along the $\langle 110 \rangle$ directions of the crystal. A chain can be seen as built from equilateral triangles sharing corners,

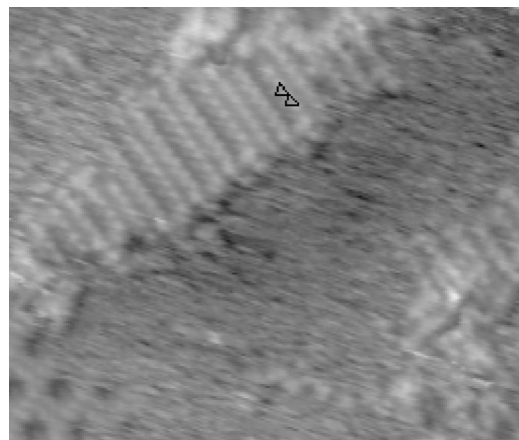


FIG. 2. S/Cu(111) at $\theta \sim 0.15$. At low temperatures chains are observed near defects and around steps. Note the different distances between chains. Two triangles with one protrusion in each corner are marked. $U = -1.00 \text{ V}$, $I = 0.170 \text{ nA}$, $T = 140 \text{ K}$, $170 \times 150 \text{ \AA}^2$.

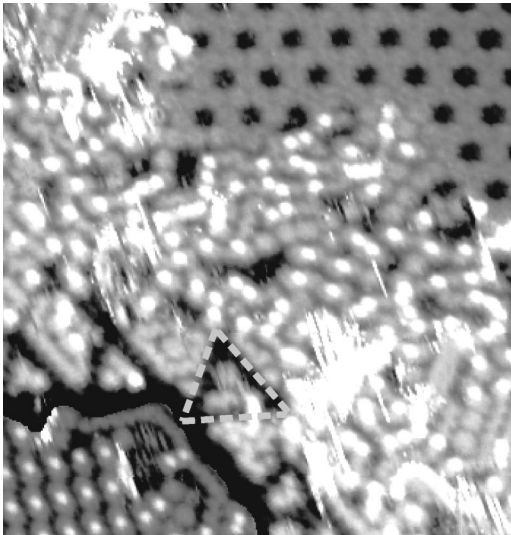


FIG. 3. S/Cu(111) at $\theta \sim 0.3$. The gray scale of the lower terrace in bottom left corner has been offset for clarity. The triangles (one of which is marked) decorating the upper step have the same height as the hc structure. Another structure labeled I, is observed in the bottom left corner (see Fig. 5). Note the high protrusions in the disordered area. $U = -1.08$ V, $I = 0.183$ nA, $T = 135$ K, $190 \times 190 \text{ \AA}^2$.

with a corner distance of 5 \AA (Fig. 2). The spacing between the chains ranges between $\sim 6 \text{ \AA}$ and $\sim 9 \text{ \AA}$. The area covered by the chains increases with decreasing temperature and increasing S coverage.

With increasing coverage a larger part of the surface is covered with the hc structure which forms islands on terraces. The appearance of the remaining, bare areas changes with temperature. At temperatures slightly below the condensation temperature of the hc structure (170 K), the bare areas resemble the RT images. The images are streaky and it is difficult to image the atomic lattice of the Cu(111) surface. When the sample is cooled further (~ 70 K) the images of the uncovered areas indicate a clean Cu(111) surface, while the center part of the triangles at edges shows the same height as the hc structure (Fig. 3).

The hc structure appears to be more stable at low temperatures (~ 70 K), but can be manipulated. If the bias voltage is set to a low value (< 0.1 V), the structure is often disrupted. Especially at the island borders it can be dissolved into smaller parts (Fig. 4).

b. $0.25 < \theta < 0.35$. In this coverage range we have observed three well-ordered structures labeled I, II, and III (Fig. 5). The areal coverage and, thus, the relative areal coverages of the different structures have not been studied in detail; hence we do not know the exact relationships between the areal coverage of the structures and temperature as well as the total sulfur exposure. However, we find that structure I is the first to coexist with the hc structure, while structures II and III are found at slightly higher coverages. The relative area the different structures cover varies a lot from terrace to terrace. A rough averaged estimate for a coverage of $\theta \sim 0.3$ shows that the hc structure covers 5% of the area and structure I 7% while structures II and III cover 10% and 4% of the area, respectively. All three of the structures can be found in different orientations, corresponding to the 12 expected

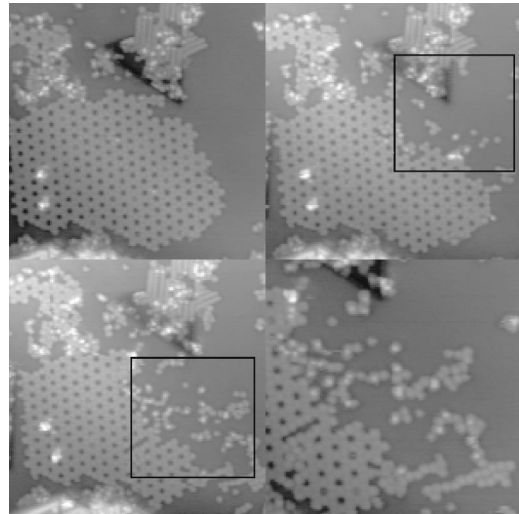


FIG. 4. S/Cu(111) at $\theta \sim 0.10$. Consecutive images of hc island, disrupted by additional low-bias images acquired between the consecutive scans. Top left: initial state. $U = -1.115$ V, $I = 0.102$ nA, $T = 60$ K, $300 \times 300 \text{ \AA}^2$. Top right: after low-bias imaging in the marked area ($U = -0.02$). $U = -1.1157$ V. Bottom left: after further low-bias imaging in the marked area. $U = -1.245$ V. Bottom right: closeup $U = -1.245$ V, $I = 0.102$ nA, $T = 60$ K, $200 \times 200 \text{ \AA}^2$.

equivalent orientations with respect to the Cu lattice for each of the structures. Structures I–III are more stable than the hc structure, and can be observed above the disordering temperature of the hc lattice (170 K). Common for I–III is that there are additional protrusions above the highest level of the hc structure, while the lower parts of the structures have the same apparent height as the hc structure. Large portions of the surface (40–80%) show a less ordered structure. These areas appear to consist of differently sized clusters of the same height as the hc structure, sometimes with protrusions similar to the ones found for I–III (Fig. 3).

One of the structures, I, has a rectangular unit cell, commensurate with the Cu(111) lattice. The unit cell, 10

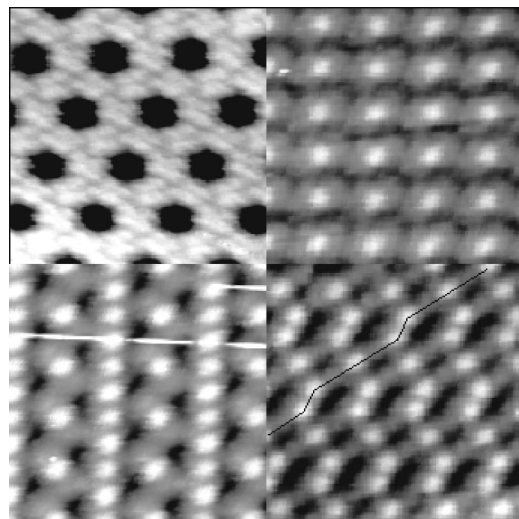


FIG. 5. Low-temperature S/Cu(111) structures. Top left: hc structure. Top right: structure I. Bottom left: structure II. Bottom right: structure III (all images $60 \times 60 \text{ \AA}^2$, $T = 135$ K).

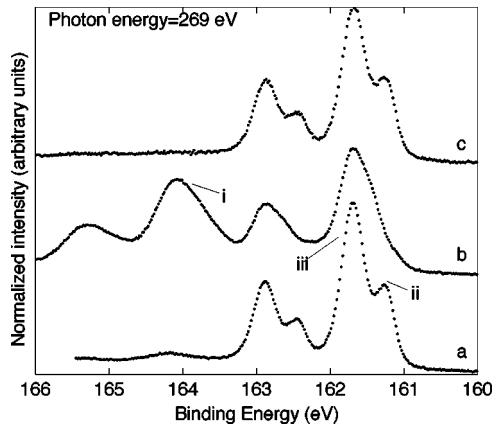


FIG. 6. Photoelectron spectra for the S $2p$ levels. (a) $(\sqrt{7} \times \sqrt{7})R \pm 19.1^\circ$ at ~ 100 K. (b) After 6 min deposition, H_2S exposure of the $(\sqrt{7} \times \sqrt{7})R \pm 19.1^\circ$ structure at ~ 100 K and $P = 2 \times 10^{-8}$ torr. (c) After heating to RT.

$\text{\AA} \times 13 \text{\AA}$, is oriented with the shorter side along the close-packed rows of the Cu(111) lattice and can be denoted $\begin{bmatrix} 4 & 0 \\ -3 & 6 \end{bmatrix}$. The unit cell contains one high protrusion.

A more complicated structure, II, can be described by a rectangular unit cell with the dimensions $22 \text{\AA} \times 11 \text{\AA}$, with the long side at an angle of 20° from one $\langle 110 \rangle$ direction. The cell fits well with a $\begin{bmatrix} 5 & -1 \\ -3 & 8 \end{bmatrix}$ unit, and contains three high protrusions. These have an apparent height of $\sim 0.4 \text{\AA}$ above the supporting structure. This is characterized by rows of protrusions along the short edges of the unit cell and parallel to the diagonal of this cell.

Yet another structure, III, can be found. Also this has three protrusions per unit cell. These fall along lines defined by the supporting structure and run $\sim 7 \text{\AA}$ from each other (Fig. 5). The line has kinks every 23\AA that fall along the $\langle 011 \rangle$ directions for $\sim 6 \text{\AA}$. The unit cell of the structure has to be repeated to coincide with the substrate lattice. A substrate unit which fits with two of the unit cells of structure III is the $\begin{bmatrix} 3 & 3 \\ -9 & 16 \end{bmatrix}$ cell.

The LEED information of main interest is that the spot pattern disappears above ~ 230 K.

B. Core level photoemission spectra

As reported previously we have used photoemission from the S $2p$ core level to monitor the number of S adsorption sites at different S coverages.⁵ In addition to this, one can obtain information of interest for a determination of the $(\sqrt{7} \times \sqrt{7})R \pm 19.1^\circ$ saturation structure. The lower spectrum of Fig. 6(a) shows two spin-orbit split $2p$ doublets for the structure. This means that the S atoms occupy at least two inequivalent sites. The spectra are recorded with the sample held at 100 K. During the cooling from RT a small amount of H_2S , residual from the deposition process, is adsorbed. The adsorbed H_2S molecules give the weak $2p_{3/2}$ peak (i) at 164.2 eV binding energy. After additional exposure to H_2S at 100 K the $2p_{3/2}$ peak due to the adsorbed molecules (i) becomes prominent (spectrum b in Fig. 6). More interestingly peak (ii) is shifted in energy while peak (iii) is unaffected by the exposure. After heating to RT only peaks (ii) and (iii) are

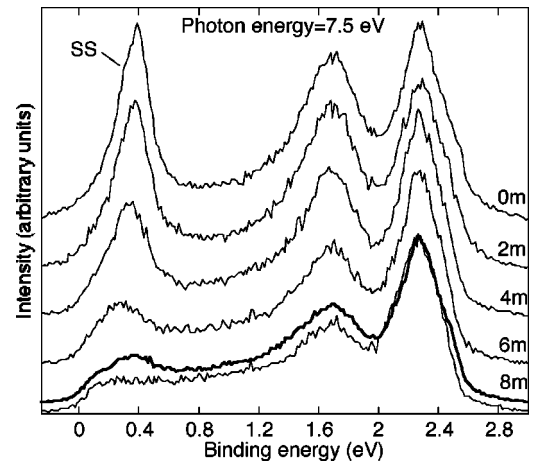


FIG. 7. Photoemission spectra from RT S/Cu(111) showing the gradual decay of the surface state photoemission peak (marked SS) with increasing coverage (fully developed hc structure corresponds to 8 min deposition at a total pressure of 2×10^{-8} torr). The bold curve is acquired after the sample has been cooled down to ~ 100 K.

detected, with the same relative intensities as prior to the additional H_2S exposure (spectrum c).

C. Valence electron spectra

1. Photoemission

To investigate how the sp band surface state of Cu(111) (Ref. 20) is affected by S deposition, we measured photoelectron spectra along the surface normal at a low photon energy (7.5 eV). Upon deposition of sulfur at RT the surface state peak, at 0.4 eV binding energy, decreases in height, and is not detected beyond a certain coverage (Fig. 7). The amount of S required to make the surface state peak vanish is nearly the same as that required to fully cover the surface with the hc structure. If the sample is then cooled (~ 100 K), a weak peak appears at nearly the same energy as observed for the surface state.

2. Scanning tunneling spectra

Scanning tunneling spectra were acquired at low temperature (~ 60 K) to avoid disruption of the hc structure. The clean areas outside the hc islands show an edge at -0.4 V due the Cu(111) surface state (Fig. 8).² When the tip is instead positioned above the hc structure there is still an enhancement above this voltage, while spectra recorded at positions above steps show no surface state feature.

IV. DISCUSSION

A. Structure models

We regard the different low-coverage structures (hc, I, II, III, and zigzag) as a family of structures. The reason for this is a number of shared characteristics. We have already described the likeness in appearance of structures I–III in the STM images, with a supporting structure on which protrusions are found. These are not only similar for all the structures, but also similar to the protrusions found in the zigzag

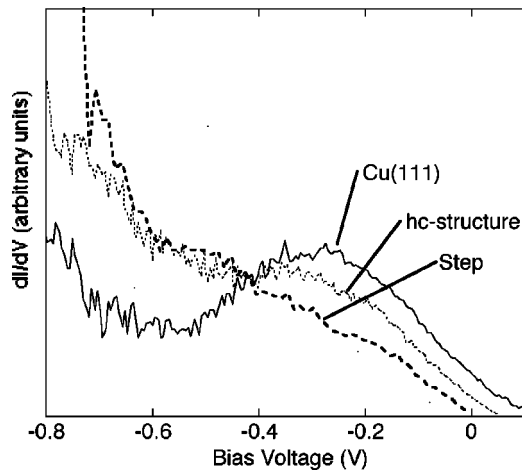


FIG. 8. Scanning tunneling spectra from S/Cu(111). The solid line is acquired above clean portions of the surface and dotted line above the hc structure, while the thick dashed line represents spectra acquired above a step. $I = 0.635$ nA, $U = -0.588$ V, $T = 60$ K.

structure. Furthermore, the S $2p$ core level spectra are similar for all the structures.⁵ Striking with the structures is the resemblance to the atomic order in the (0001) cleavage plane of CuS (covellite). In this plane the two elements occupy alternating sites to form a honeycomb pattern (Fig. 9).^{21,22} In particular, for the hc structure, the positions of the protrusions are almost identical to those for S or Cu atoms in covellite (0001), except for seven missing protrusions per unit cell. If every protrusion in the hc structure is thought of as an S atom, there will be 12 S atoms in the unit cell, which covers 43 Cu atoms, rendering a coverage of 0.28, close to the observed saturation coverage of the hc structure. The identification of the protrusions as S atoms finds support in a recent STM investigation, which has shown that only the S atoms in the CuS cleavage plane are imaged.²²

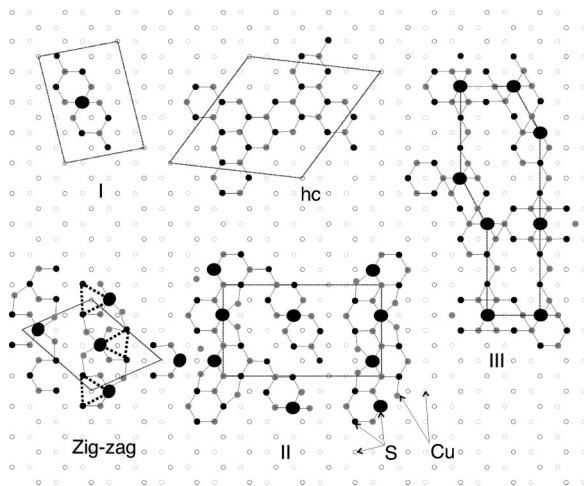


FIG. 9. Models of the different low-coverage structures found at S/Cu(111). The background lattice shows a covellite layer for comparison, with alternating rings marking S or Cu. Solid rings: surface structure atoms. Small black rings: S. Gray rings: copper. The large solid black rings mark the position of a S atom coordinated to four Cu in-plane atoms, interpreted as protrusions in the STM images. Possible bonds and unit cells are marked by solid lines.

Furthermore, the coincidence pattern between the Cu(111) lattice and a covellite layer is identical to the unit cell found for the hc structure [close-packed rows of S atoms rotated by 15° with respect to $\langle 011 \rangle$ in Cu(111)]. We also find that structures I, II, and III have unit cells which match well with CuS/Cu(111) coincidence patterns.

Even the zigzag pattern matches well with a covellite plane along the zigzag lines. In Fig. 9 the basic features of this structure are shown. Foss *et al.*⁷ suggest that the protrusions observed in the STM images are due to S atoms which are coordinated to four in-plane Cu atoms to form a Cu_4S cluster, with the S atom residing in the hollow above the four Cu atoms. As Fig. 9 shows the structure model by Foss *et al.* can be interpreted in terms of a covellite structure where triangles (marked in Fig. 9) of the CuS structure are positioned in rows so that every third S atom has four Cu neighbors and can form a protruding Cu_4S cluster.

In the same manner structures I, II, and III can be described as reordered covellite layers. Structure I can be described by two Cu_3S_3 clusters joined with a sulfur atom which forms a protrusion. Both the angle and size of the structure fit well with our observations. The unit cell covers 24 substrate atoms, which with seven S atoms renders a coverage of 0.29. This value is within the interval of $0.28 < \theta < 0.35$, where the lower limit is set by assuming 12 S atoms per 43 Cu atoms of the hc structure. The upper coverage limit is set by the zigzag structure which contains 6 S atoms per 17 Cu surface atoms.⁷

For the structures with larger unit cells, the models proposed here are tentative. Structure II can be thought of as rows of a zigzag pattern with the units found in structure I between them. This renders a unit cell with three protrusions in the right location. The unit cell covers 42 Cu atoms and 13 S atoms, giving a coverage of 0.31, again within the expected interval.

We also present a tentative structure model for structure III, which reproduces both the locations of the protrusions and the supporting structure with the right periodicity. This unit cell has to be repeated twice to be commensurate with the substrate unit cell which contains 81 Cu atoms, which with 28 S atoms gives a coverage of 0.345. This is close to the coverage of the zigzag structure.

For the hc structure there is, as stated above, a good match between the observed protrusions and the positions of the S atoms in a covellite layer, given that seven S atoms are removed in every unit cell. Thus the depressions seen in the images can be interpreted as holes without any adsorbate atoms. An obvious interpretation of the valence electron spectra is also that the holes in the hc structure seem to be free of adsorbed atoms, as they show that the surface state actually regains intensity as the structure is formed. We ascribe the gain in intensity to the formation of bare Cu(111) areas. The scanning tunneling spectra show that the regained intensity originates at least partly from the hc structure, and is not entirely due to open areas obtained when the hc phase orders. As only clean Cu(111) surfaces are expected to support a surface state at the same energy, it is probable that the holes in the structure actually are areas with a rather undistorted Cu(111) lattice.

It is not uncommon for a sulfur adsorption system to show a large number of complex phases which often show similar structures; it can therefore be interesting to compare the S/Cu(111) system with other sulfur adsorption systems. Thoroughly investigated is the S/Ru(0001) system which displays five commensurate phases.^{17,23} However, in contrast to the low-coverage hc structure found for S/Cu(111), the low-coverage phase is a $p(2 \times 2)$ overlayer, which cannot share the openness of the hc structure. Further examples often referred to in connection to the S/Cu(111) are the S/Pd(111) and S/Ag(111) systems. The S/Pd(111) system shows a $(\sqrt{3} \times \sqrt{3})R \pm 30^\circ$ structure and (2×2) stripelike structures at low coverages,^{15,16,24} while S/Ag(111) displays LEED patterns indicating a more complicated family of structures which have not been fully determined.^{14,25} It is interesting to note that although all of the mentioned systems show a $(\sqrt{7} \times \sqrt{7})R \pm 19.1^\circ$ structure, the suggested structure models have all the adsorbate atoms in the top layer, contrary to the model of the Cu(111)- $(\sqrt{7} \times \sqrt{7})R \pm 19.1^\circ$ -S structure presented by Foss *et al.*⁷ and favored by our data. Thus the S/Pd(111) system and the S/Ru(0001) system, often mentioned as closely related to S/Cu(111), might not be as closely related. However, to us, the S/Ag(111) system has not been thoroughly investigated; accordingly further investigations of this system might reveal similarities to the S/Cu(111) system.

B. Building blocks of the structures

The hc structure is a phase formed by condensation of atoms or clusters that are mobile at RT. The RT study of step etching performed by Ruan *et al.*¹⁰ indicates the formation of clusters by which Cu is transported from the edges. Another indication of cluster formation is that the S $2p$ core level spectra show little change upon condensation of the structures; thus the sulfur must be bound in a similar manner both in the formed structures and the building blocks diffusing at RT.⁵

If clusters are the building blocks, these may be the ones proposed by Feibelman,¹⁸ which share their internal structure with the chains and triangles formed close to dislocations and step edges (Figs. 1 and 3). However, none of the extended structures presented here have any features that suggest Cu_3S_3 as building units. We cannot determine the nature of the diffusing species, as we can only observe the condensed products which have two different types of order: 2×2 (step edges, triangles) or covellite like (hc, I, II, and III).

C. Step edge and defect decorations

According to our images the decoration of edges is specific to the orientation of the step edge. This means that decoration is specific to the type of step edge [*A* type, (100) microfacets, or *B* type, (110) microfacets], leaving either an edge decorated by a row of protrusions or an edge indented with triangles (Fig. 1).

Common for both the protrusions at edges and the chains is the 2×2 ordering. It is interesting to note that this order

resembles the Cu_3S_3 clusters.¹⁸ It seems plausible that the chains and the more complex structures found at and close to the triangles (Fig. 3) are built from Cu_3S_3 clusters. That a local ordering is observed near imperfections would then suggest that these provide more stable sites for the clusters than does an open terrace.

D. Honeycomb structure

The striking property of the hc structure is the holes formed in what otherwise seems to be a covellite layer. This is interesting since the structure forms at low T via the ordering of adsorbed species. One of the intentions of this study was to elucidate the processes responsible for the openness of the hc structure. An obvious reason could be the mismatch between a covellite layer and the Cu substrate: a large local mismatch might result in abandoned sites. However, upon examining the mismatch we find that the large difference in period (1.5/1) together with the rotation (15°) rendered a mismatch without any resemblance to the holes in the structure.

Another plausible cause for the openness is an elastic deformation of the substrate lattice. This is known to mediate forces at long range and could possibly block the hollows for growth.²⁶ An interaction can also be mediated by the surface state present in the open areas.^{27,4} This would form a structure with a periodicity with a length scale of roughly one Friedel oscillation. For the Cu(111) surface state the period of oscillation is 15 \AA and this is close to the structure period 16.7 \AA .

E. $(\sqrt{7} \times \sqrt{7})R \pm 19.1^\circ$

The Cu(111)- $(\sqrt{7} \times \sqrt{7})R \pm 19.1^\circ$ -S structure has attracted considerable attention. The model put forward by Foss *et al.*⁷ was recently rejected by Saily and Mitchell¹² on the basis of a LEED analysis, but favored in the study by Jackson *et al.*¹³ In the model by Foss *et al.* the top layer consists of Cu_4S clusters, with the S atom in the hollow above four in-plane Cu atoms. Beneath this tetramer there are two buried S atoms. In the recent model by Saily and Mitchell two S atoms take positions in same plane as the top Cu atoms, while the third S atom is buried below the topmost Cu layer.

A straightforward interpretation of the core level data (Fig. 6) is that the high-intensity peak (iii) is associated with the S atoms which occupy two nearly equivalent sites per unit cell, while the low-intensity peak (ii) is associated with the S atoms occupying one site per unit cell. It is also an obvious interpretation that peak (ii) originates from sites that are highly affected by the presence of adsorbed molecular H_2S . Thus, the data support the model by Foss *et al.* as the two subsurface atoms per unit cell would render the high-intensity peak (iii) insensitive to adsorption while the surface S atom would give a weaker peak (ii), more sensitive to adsorbed species.

V. CONCLUSIONS

A number of low-temperature and low-coverage structures of S/Cu(111) have been found. Four phases which crystallize below RT are described. In addition local rearrangements are found near steps and defects. The structures formed have two different geometries. One type is a 2×2 ordering found locally near steps and dislocations. The extended low- T structures of S/Cu(111) can be described by a local order which resembles that of covellite (0001) planes.

Especially the hc structure is a good match to this. The higher-coverage structures I, II, and III can be described in the same manner but with a reordering of the covellite layer. The honeycomb lattice is found to support the surface state characteristic of the clean Cu(111) surface. We attribute the openness of the honeycomb lattice to long-ranged forces mediated by the substrate. Core level photoemission data provide for a structure model for Cu(111)- $(\sqrt{7} \times \sqrt{7})R \pm 19.1^\circ$ -S proposed by Foss *et al.*⁷

-
- ¹Y. Hasegawa and P. Avouris, Phys. Rev. Lett. **71**, 1071 (1993).
²M. Crommie, C. Lutz, and D. Eigler, Nature (London) **363**, 524 (1993).
³B. Hinch, J. Frenken, G. Zhang, and J. Toennies, Surf. Sci. **259**, 288 (1991).
⁴E. Wahlström, I. Ekvall, H. Olin, and L. Walldén, Appl. Phys. **66**, S1107 (1998).
⁵E. Wahlström, I. Ekvall, H. Olin, S.-Å. Lindgren, and L. Walldén, Phys. Rev. B **60**, 10699 (1999).
⁶J. Domange and J. Oudar, Surf. Sci. **11**, 124 (1968).
⁷M. Foss, R. Feidenhansl, M. Nielsen, E. Findeisen, T. Buslaps, R. Johnson, and F. Besenbacher, Surf. Sci. **388**, 5 (1997).
⁸C. Campbell and B. Koel, Surf. Sci. **183**, 100 (1987).
⁹N. Prince, D. Seymore, M. Aswin, C. McConville, and D. Woodruff, Surf. Sci. **230**, 13 (1990).
¹⁰L. Ruan, I. Stensgaard, F. Besenbacher, and E. Lægsgaard, Ultramicroscopy **42-44**, 498 (1992).
¹¹K. Motai, T. Hushizume, H. Lu, D. Jeon, and T. Sakurai, Appl. Surf. Sci. **67**, 246 (1993).
¹²M. Saily and K. Mitchell, Surf. Sci. **441**, 425 (1999).
¹³G. Jackson, S. Driver, D. Woodruff, B. Cowie, and R. Jones, Surf. Sci. **453**, 183 (2000).
¹⁴G. Rovida and F. Pratesi, Surf. Sci. **104**, 609 (1981).
¹⁵M. Frantisek and M. Scheffler, Surf. Sci. **160**, 467 (1985).
¹⁶S. Speller, T. Rauch, J. Bömermann, P. Borrmann, and W. Heiland, Surf. Sci. **441**, 107 (1999).
¹⁷R. Dennert, M. Sokolowski, and H. Pfnür, Surf. Sci. **271**, 1 (1992).
¹⁸P. Feibelman, Phys. Rev. Lett. **85**, 606 (2000).
¹⁹I. Ekvall, E. Wahlström, D. Claesson, H. Olin, and E. Olsson, Meas. Sci. Technol. **10**, 11 (1999).
²⁰P. Gartland and B. Slagsvold, Phys. Rev. B **12**, 4047 (1975).
²¹S. Djurle, Acta Chem. Scand. **12**, 1415 (1958).
²²K. Rosso and J.M.F. Hochella, Surf. Sci. **423**, 364 (1999).
²³W. Sklarek, C. Schwennicke, D. Jürgens, and H. Pfnür, Surf. Sci. **330**, 11 (1995).
²⁴W. Liu, K. Mitchell, and W. Berndt, Surf. Sci. **393**, L119 (1997).
²⁵K. Schwaha, N. Spenser, and R. Lambert, Surf. Sci. **81**, 273 (1979).
²⁶K. Lau and W. Kohn, Surf. Sci. **65**, 607 (1977).
²⁷K. Lau and W. Kohn, Surf. Sci. **75**, 69 (1978).